HYDRONETS: LEVERAGING RIVER STRUCTURE FOR HYDROLOGIC MODELING

Anonymous authors
Paper under double-blind review

ABSTRACT

Accurate and scalable hydrologic models are essential building blocks of several important applications, from water resource management to timely flood warnings. However, as the climate changes, precipitation and rainfall-runoff pattern variations become more extreme, and accurate training data that can account for the resulting distributional shifts become more scarce. In this work we present a novel family of hydrologic models, called HydroNets, which leverages river network structure. HydroNets are deep neural network models designed to exploit both basin specific rainfall-runoff signals, and upstream network dynamics, which can lead to improved predictions at longer horizons. The injection of the river structure prior knowledge reduces sample complexity and allows for scalable and more accurate hydrologic modeling even with only a few years of data. We present an empirical study over two large basins in India that convincingly support the proposed model and its advantages.

1 INTRODUCTION

Prior knowledge plays an important role in machine learning and AI. On one extreme of the spectrum there are expert systems, which exclusively rely on domain expertise encoded into a model. On the other extreme there are general purpose methods, which are exclusively data-driven. In the context of hydrologic modeling, conceptual models such as the Sacramento Soil Moisture Accounting Model (SAC-SMA) (Burnash et al., 1973), are analogues to expert systems and require explicit functional modeling of water volume flow. Instances of agnostic methods have recently been presented by Kratzert et al. (2018; 2019) and by Shalev et al. (2019), showing that general purpose deep recurrent neural networks can achieve state-of-the-art hydrologic forecasts at scale.

Global climate changes resulting in new weather patterns can cause rapid distributional shifts that make learned models irrelevant. In particular, relevant or recent data is scarce by definition and learning from such data can lead to substantial overfitting. Our goal in this work is to incorporate useful prior knowledge into machine learned hydrologic models so as to overcome this obstacle.

We present *HydroNets*, a family of deep neural network models designed for hydrologic forecasting. HydroNets leverages the prior knowledge of the sub-basins' structure of a hydrologic region. HydroNets also enforce some weight sharing between sub-basins, resulting in a shared model and basin-specific models that correspond to the general-physical hydrologic modeling which is shared among basins vs. the basin-specific modeling that account for basin properties. The proposed architecture is modular, thus making it convenient to understand and improve. We present experimental results over two regions in India which convincingly show that the proposed model utilizes learning examples from the whole region, avoids overfitting, and performs better when training data is scarce.

2 PROBLEM SETTING

We define a *hydrologic region* $\mathcal{R}$ to be a directed graph, $\mathcal{R} = (\mathcal{B}, \mathcal{E})$, where each node in the node set, $\mathcal{B} = \{b_1, \ldots, b_n\}$, represents a basin and each directed edge, $b_i \rightarrow b_j \in \mathcal{E}$, indicates that b_i is a direct sub-basin of b_j. An edge direction corresponds to water flow from a sub-basin to its containing basin, and whenever an edge $b_i \rightarrow b_j$ exists we say that b_i is a *source* of b_j (there can be multiple sources), and b_j is the *downstream* node of b_i. A basin whose out-

degree is zero is called a *region drain*. A basin without sources (whose in-degree is zero) is called a *region source*. For each basin $b \in B$ we denote by $S(b) \subseteq B$ the set of sources of b.

Naturally, due to the topological properties of rivers, sub-basins' structure span an "inverted tree". Figure-1 shows an example for such a hydrologic region.

For each basin b_i we consider a sequence of its *temporal features*, $\mathcal{X}_i^{1:t} \triangleq \mathbf{x}_i^{(1)}, \mathbf{x}_i^{(2)}, \ldots, \mathbf{x}_i^{(t)}$, where $\mathbf{x}_i^{(t)}$ is the feature vector of time t, which can include features such as *precipitation*, *temperature*, past readings of the gauge itself, and so on. For each basin, we also include a vector, $\mathbf{z}_i$, of *static features*, which are specific to basin i and are fixed through time. Such feature can include soil type, elevation, etc..

Figure 1: Hydrologic region example

For each basin b_i, let $\mathbf{y}_i^{1:t}$ be its *target label* sequence. Typically, target labels are *water-levels* or *discharges* (i.e., the volumetric flow rate of water). Given a desired prediction horizon, h (say, two days), the task is to create model $F_{\mathcal{R}}$ for region $\mathcal{R}$ that accurately forecasts the target labels of all basins at horizon h from a past window of inputs of length T (e.g., a month), $F(\mathcal{X}_1^{(t-T:t)}, \ldots, \mathcal{X}_n^{(t-T:t)}, \mathbf{z}_1, \ldots, \mathbf{z}_n) \to (y_1^{t+h}, \ldots, y_n^{t+h})$. In hydrologic forecasting, prediction quality is traditionally measured using the Nash–Sutcliffe efficiency (NSE) (Nash & Sutcliffe, 1970), which is equivalent to the R^2 ("variance explained") of classical statistics. In this work we will also use the R^2-persist metric as defined in Appendix-A.
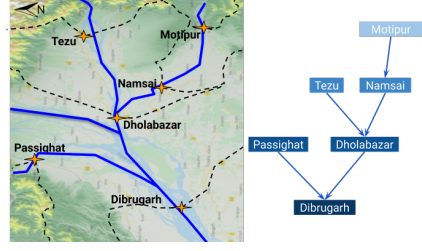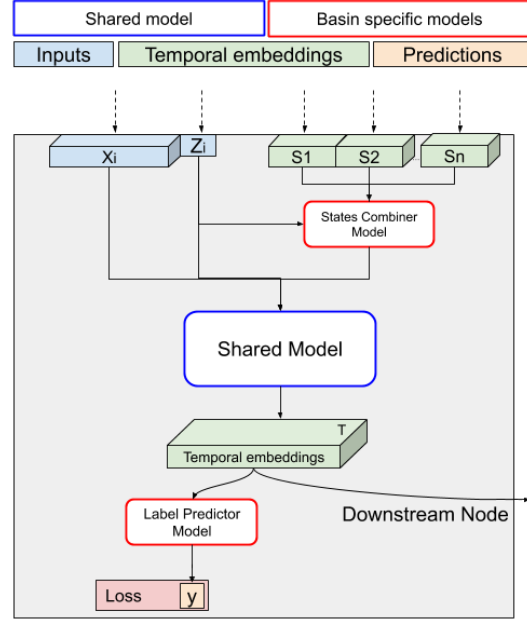
3 HYDRONETS

We propose a novel family of architectures for hydrologic forecasting. Models in this family, called *HydroNets*, leverage the prior information provided by the river's structure. Given a hydrologic region $\mathcal{R} = (\mathcal{B}, \mathcal{E})$, HydroNets spans a computation graph that follows $\mathcal{R}$ such that for every basin $b_i \in \mathcal{B}$ in the river graph, the network, $H(\mathcal{R}) \triangleq (H_1, \ldots, H_n)$, contains a sub-network (also called a *node*) H_i. H_i is connected to H_j iff $(b_i \to b_j) \in \mathcal{E}$. Each node H_i is composed of three sub-models, two of which are basin-specific and the third is shared among all basins. The role of these sub-models is explained below. In each node b_i, the shared model outputs a *temporal embedding* vector which encodes self and upstream information for this basin. Additionally, making use of this embedding, a basin-specific model outputs the target label (e.g., water level) at basin b_i. All nodes, other than the region's drain basin, pass their temporal embeddings to their downstream node. We define $K \triangleq |E_i^{(t)}|$, the size of every embedding vector and consider it as a hyperparameter of the network. We now describe each of the three sub-models. Functional forms are given in Figure 2.

$$F_i^{\text{CMB}}\left(\left\{ E_j^{(t-T:t)} \mid j \in S(b_i) \right\}, \mathbf{z}_i\right) \to C_i^{(t-T:t)}$$

$$F^{\text{SHA}}\left(\mathcal{X}_i^{(t-T:t)}, \mathbf{z}_i, C_i^{(t-T:t)}\right) \to E_i^{(t-T:t)}$$

$$F_i^{\text{PRD}}\left(E_i^{(t-T:t)}\right) \to l_i^{(t+h)}$$

Figure 2: HydroNets Architecture

Combiner. Each basin b_i receives as input its static features vector, $\mathbf{z}_i$, as well as all the temporal embedding of its sources in $S(b_i)$. These inputs are fed to a basin-specific sub-model, F_i^{CMB}, called

combiner. The output of the combiner is a $T \times K$ matrix, denoted $C_i^{(t-T:t)}$. The combiner allows each node to handle a different number of sources, and moreover, allows the node to account for the relative importance of its sources, which depend on the distances to the sources, relative water volume of the sources, and so on.

Shared Hydrologic Model. The basin-specific output of the combiner at each node, $C_i^{(t-T:t)}$, as well as its temporal and static features, $(\mathcal{X}_i^{(t-T:t)}, \mathbf{z}_i)$, are fed as inputs to a shared model F^{SHA}. This model computes the temporal embeddings for this node and its output is a $T \times K$ matrix $E_i^{(t-T:t)}$.

Basin-Specific Prediction Model. Based on the temporal embeddings of node i, its basin-specific prediction model, denoted F_i^{PRD}, predicts the target label at time $t + h$. This allows HydroNets to account for basin-specific behavior.

Figure 2 depicts a single node in the HydroNets architecture. HydroNets recursively builds such nodes by traversing the graph $\mathcal{R}$ starting with the region drain. The resulting computational graph is thus a tree that matches $\mathcal{R}$. The loss function used to optimize our model is a weighted sum over all *MSE* terms between every l_i and its corresponding y_i.

4 EMPIRICAL STUDY

In the empirical study presented here, we instantiated HydroNets such that all sub-models are linear. The handling of temporal embedding vectors by each of these sub-models is done such that the same weights are used on all time steps. Throughout our study, we use the following *flat linear* baseline predictor which does not utilize the hydrologic structure (i.e., concatenates the features). Note that our implementation of HydroNets (and the baseline) does not include static features.

The Ganga and Brahmaputra Datasest. The datasets used in our experimental study were constructed from two main sources. For precipitation we relied on JAXA's GSMap satellite (Ushio et al., 2003), which generates hourly images of rainfall intensity. Water level measurements were taken from the Indian Central Water Commission. For this study we constructed two sub-regions from the Brahmaputra and the Ganga rivers. More detailed maps are in Appendix-B.
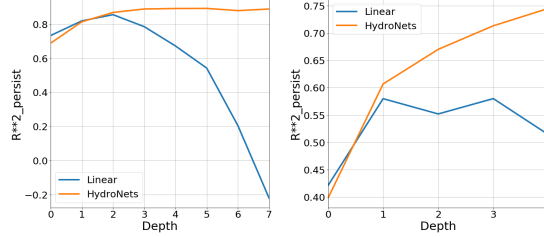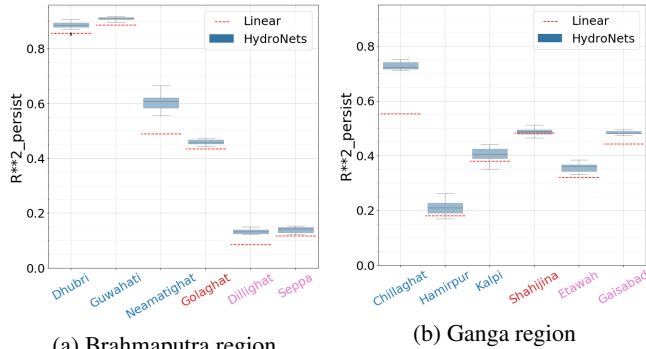

(a) Brahmaputra region   (b) Ganga region

Figure 3: R-squared on different tree depths

We extracted the polygon describing each basin's geo-spatial location using the HydroSHEDS datasets (Lehner et al., 2008; Lehner & Grill, 2013) and calculated the lumped average rain intensity over the basin. Every example (i.e., timestamp) in the dataset contains a historical window of length T of the precipitation and past water-levels as the features, and the measurement at $t + h$ as the label. Our dataset contains five monsoon periods (Jun to Oct) during the years 2014 to 2018. We used the first four years for training and the last one for testing.

Experiment 1: The Value of Depth. We consider the effect of using trees of different depths on prediction at the drain basin of each region. The R^2-persist metric results are presented in Figure 3 where we observe that initially both models gain from deepening the tree but while the baseline model starts deteriorating, the HydroNets model keeps leveraging information from deeper branches. Qualitatively similar results with the standard R^2 metric are presented in Appendix-D.

(a) Brahmaputra region   (b) Ganga region

Figure 4: Persist R-squared on different basins

3

Experiment 2: All Basins Comparison. We examine the performance of HydroNets in each region relative to the flat linear baseline at all sites. For each basin, we trained a different model where the loss weights were heavily adjusted towards this basin. The flat model was trained for every basin separately with a depth of 2 (following our previous experiment).

We selected 6 representative basins from each region, based on a hydrologic context, where we balanced between large basins where the gauges are located on the main rivers, and smaller upstream basins, which are region sources (leaves) in the region graph. Figure 4 visualizes average results over 10 random initializations and shows that HydroNets outperforms the flat linear baseline in all 6 representative basins. We also see that some basins are harder to predict than the others. This tends to be the case with the more up-stream basins. Appendix-C presents the results for all sub-basins in both regions, where HydroNets outperforms the flat linear model in a large majority of cases, and provides comparable performance in the rest.

Experiment 3: Learning from fewer samples. We examine the performance achieved using a significantly smaller training set. Instead of utilizing the entire four years in our datasets, in this study we present forecasting performance when using only the last years for training. In all cases, the test set is fixed to be the fifth year in our datasets. The results indicate that HydroNets has a substantial and increasing advantage over the flat linear baseline when the training set becomes smaller. Figure 5 shows the results for three examples of sub-basins.
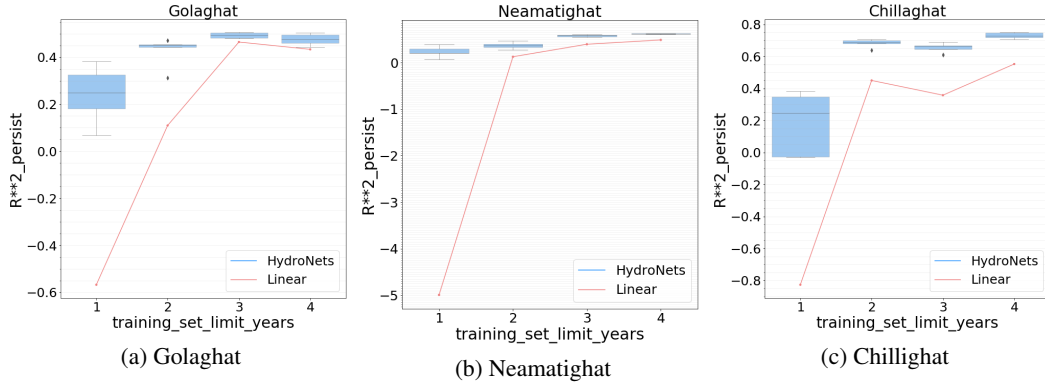

(a) Golaghat   (b) Neamatighat   (c) Chillighat

Figure 5: R^2-persist when increasing number of training years

5 RELATED WORK

Up to date, most hydrologic models are physical models such as SAC-SMA (Burnash et al., 1973) and WRF-hydro (Salas et al., 2018). Kratzert et al. (2019) presented a regional model for hundreds of gauged basins that strongly depends on basin-specific static features such as area, soil type, etc. and exhibited state-of-the-art streamflow forecasting performance. While in the work of Kratzert et al. (2019) the network used static catchment attributes derived from gridded data products, Shalev et al. (2019) showed that in the fully gauged setting the same model can be used without static catchment attributes but with a learned site embedding.

6 CONCLUDING REMARKS

We presented HydroNets, a family of architectures for hydrologic modeling. A distinct advantage of the HydroNets architecture is that it reduces the sample complexity. This property enables forecasting in basins where training data is scarce, or when patterns change rapidly, perhaps due to climate change. HydroNets is a flexible family of models and in this work we only considered linear instantiations of its sub-models. Future work may include non-linear and recurrent sub-models, experimenting in other regions, working with discharge as the label and adding static basin features to the implementation.

REFERENCES

Robert JC Burnash, R Larry Ferral, and Robert A McGuire. *A generalized streamflow simulation system: Conceptual modeling for digital computers*. US Department of Commerce, National Weather Service, and State of California, 1973.

Frederik Kratzert, Daniel Klotz, Claire Brenner, Karsten Schulz, and Mathew Herrnegger. Rainfall–runoff modelling using long short-term memory (lstm) networks. *Hydrology and Earth System Sciences*, 22(11):6005–6022, 2018.

Frederik Kratzert, Daniel Klotz, Guy Shalev, Günter Klambauer, Sepp Hochreiter, and G Nearing. Towards learning universal, regional, and local hydrological behaviors via machine learning applied to large-sample datasets. *Hydrology and Earth System Sciences*, 23(12):5089–5110, 2019.

Bernhard Lehner and Günther Grill. Global river hydrography and network routing: baseline data and new approaches to study the world's large river systems. *Hydrological Processes*, 27(15): 2171–2186, 2013.

Bernhard Lehner, Kristine Verdin, and Andy Jarvis. New global hydrography derived from space-borne elevation data. *Eos, Transactions American Geophysical Union*, 89(10):93–94, 2008.

J Eamonn Nash and Jonh V Sutcliffe. River flow forecasting through conceptual models part i—a discussion of principles. *Journal of hydrology*, 10(3):282–290, 1970.

Fernando R Salas, Marcelo A Somos-Valenzuela, Aubrey Dugger, David R Maidment, David J Gochis, Cédric H David, Wei Yu, Deng Ding, Edward P Clark, and Nawajish Noman. Towards real-time continental scale streamflow simulation in continuous and discrete space. *JAWRA Journal of the American Water Resources Association*, 54(1):7–27, 2018.

Guy Shalev, Ran El-Yaniv, Daniel Klotz, Frederik Kratzert, Asher Metzger, and Sella Nevo. Accurate hydrologic modeling using less information. *Machine Learning and the Physical Sciences, NeurIPS*, 2019.

Tomoo Ushio, Ken'ichi Okamoto, Toshio Iguchi, Nobuhiro Takahashi, Koyuru Iwanami, Kazumasa Aonashi, Shoichi Shige, Hiroshi Hashizume, Takuji Kubota, and Toshiro Inoue. The global satellite mapping of precipitation (gsmap) project. *Aqua (AMSR-E)*, 2004, 2003.

A DEFINING THE R^2-PERSIST METRIC

In this work we introduce and utilize a performance metric, which we term R^2-*persist*. Both the standard R^2 metric, a.k.a. Nash–Sutcliffe efficiency (NSE) (Nash & Sutcliffe, 1970), and the proposed R^2-persist metric have the same general form as a ratio between the mean squared error (MSE) of the model's prediction, relative to the MSE of the predictions of a baseline,

$$1 - \frac{\text{MSE}(\mathcal{F}_{\mathcal{R}})}{\text{MSE}(\text{BASELINE})}$$

In the *NSE* (R^2) metric, the baseline is taken to be the average predicted value, while in the R^2-persist metric, the baseline is a naive model that always predicts the future using the present reading of the target label measurement (i.e., $\hat{y}_i^{t+h} = y_i^t$).

The motivation for introducing this new metric is that in large rivers, the persist baseline is a much stronger model than the average baseline, which makes the R^2-persist a more challenging and meaningful performance measure. The values of both metrics are in the interval $(-\infty, 1]$, and near zero values reflect baseline performance.

B DETAILED MAPS OF THE TWO REGIONS

Figure 6 shows the two hydrologic regions we used to construct the Brahmaputra and Ganga datasets that were used in our empirical study. Both regions are in India, where the Brahmaputra region is located in the east part of the Brahmaputra river, and the Ganga region is a small part of the whole Ganga basin, which is located near the city of Lucknow.
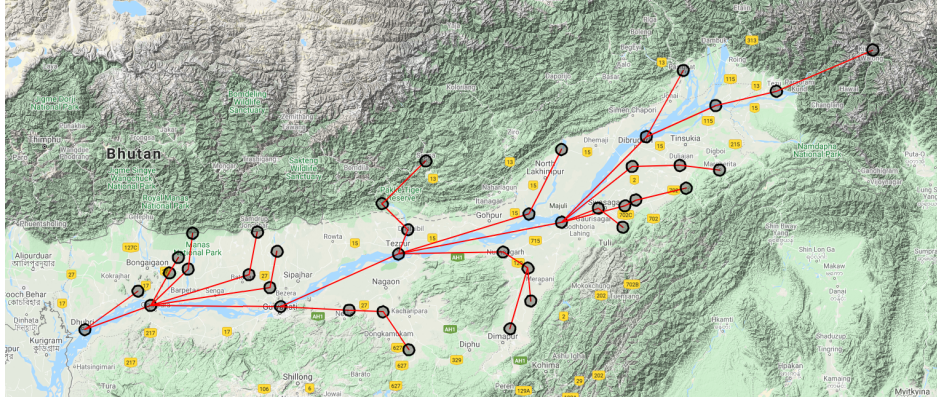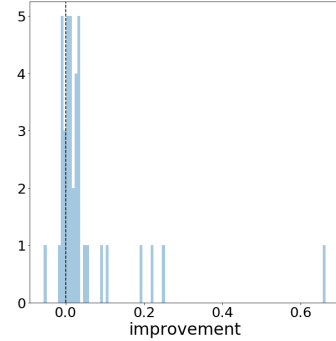

(a) Brahmaputra region
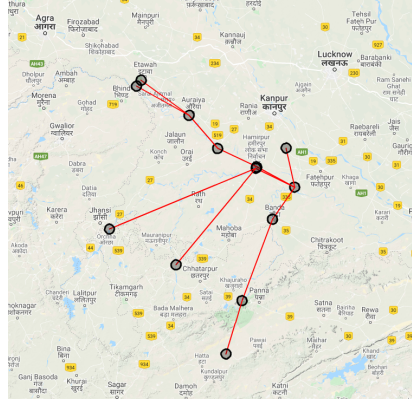
(b) Ganga region

Figure 6: The Brahmaputra and the Ganga regions

C RESULTS OVER ALL BASINS

Table 1 shows the results of Experiment 2 for all basins in both regions. The table shows the R^2-persist metric. For each region we also present a histogram of the *diff* column values. As can be seen, the HydroNets model outperforms the linear model in a large majority of basins.

Brahmaputra				Ganga			
Basin Name	Linear	HydroNets	Diff	Basin Name	Linear	HydroNets	Diff
Badatighat	0.557	0.566	0.009	Auralya	0.305	0.292	0.012
Behalpur	0.321	0.329	0.008	Banda	0.684	0.671	0.013
Beki Road bridge	0.142	0.174	0.032	Chillaghat	0.735	0.552	0.183
Bhalukpong	−0.055	0.163	0.218	Etawah	0.349	0.320	0.029
Bihubar	0.276	0.272	−0.003	Gaisabad	0.482	0.443	0.040
Bokajan	0.317	0.329	0.012	Garrauli	0.519	0.495	0.025
Chenimari	0.720	0.701	−0.019	Hamirpur	0.177	0.179	−0.002
Chouldhowaghat	0.255	0.254	−0.001	Kalpi	0.420	0.379	0.041
Desangpani	0.378	0.400	0.022	Kora	−0.053	−0.542	0.489
Dharamtul	0.551	0.562	0.011	Madla	0.495	0.458	0.038
Dholabazar	−1.365	−1.118	0.247	Nautghat	0.348	0.304	0.044
Dhubri	0.855	0.865	0.010	Shahijina	0.477	0.482	−0.006
Dibrugarh	−0.440	0.223	0.663	Udi	0.397	0.399	−0.002
Dillighat	0.085	0.137	0.052				
Gelabil	0.101	0.130	0.028				
Goalpara	0.851	0.861	0.009				
Golaghat	0.433	0.467	0.034				
Guwahati	0.886	0.911	0.025				
Jiabharali NT . . .	−0.014	0.182	0.196				
Kampur	0.504	0.538	0.034				
Kheronighat	0.537	0.566	0.029				
Kibithu	0.119	0.130	0.011				
Manas NH . . .	0.298	0.320	0.022				
Margherita	0.178	0.167	−0.011				
Mathanguri	0.159	0.163	0.004				
Matunga	0.050	0.098	0.048				
Naharkatia	0.317	0.307	−0.009				
Nanglamoraghat	0.586	0.577	−0.008				
Neamatighat	0.487	0.596	0.109				
Numaligarh	0.548	0.542	−0.006				
Pagladiya . . .	0.208	0.245	0.036				
Panbari	0.245	0.245	0.000				
Passighat	0.059	0.150	0.091				
Puthimari . . .	0.250	0.282	0.032				
Seppa	0.116	0.145	0.028				
Sivasagar	0.360	0.368	0.008				
Suklai	0.237	0.241	0.004				
Tezpur	0.842	0.786	−0.056				
Tezu	0.118	0.108	−0.010				

Brahmaputra Improvement (Diff)
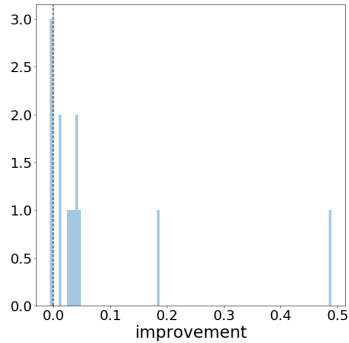

Ganga Improvement (Diff)

Table 1: Full results over all basins in the Brahmaputra and Ganga regions.

D R^2 RESULTS

In Figure 3 and Figure 4 we presented the results of Experiment 1 using the R^2-persist metric. Following are the R^2 results for the same experiment.
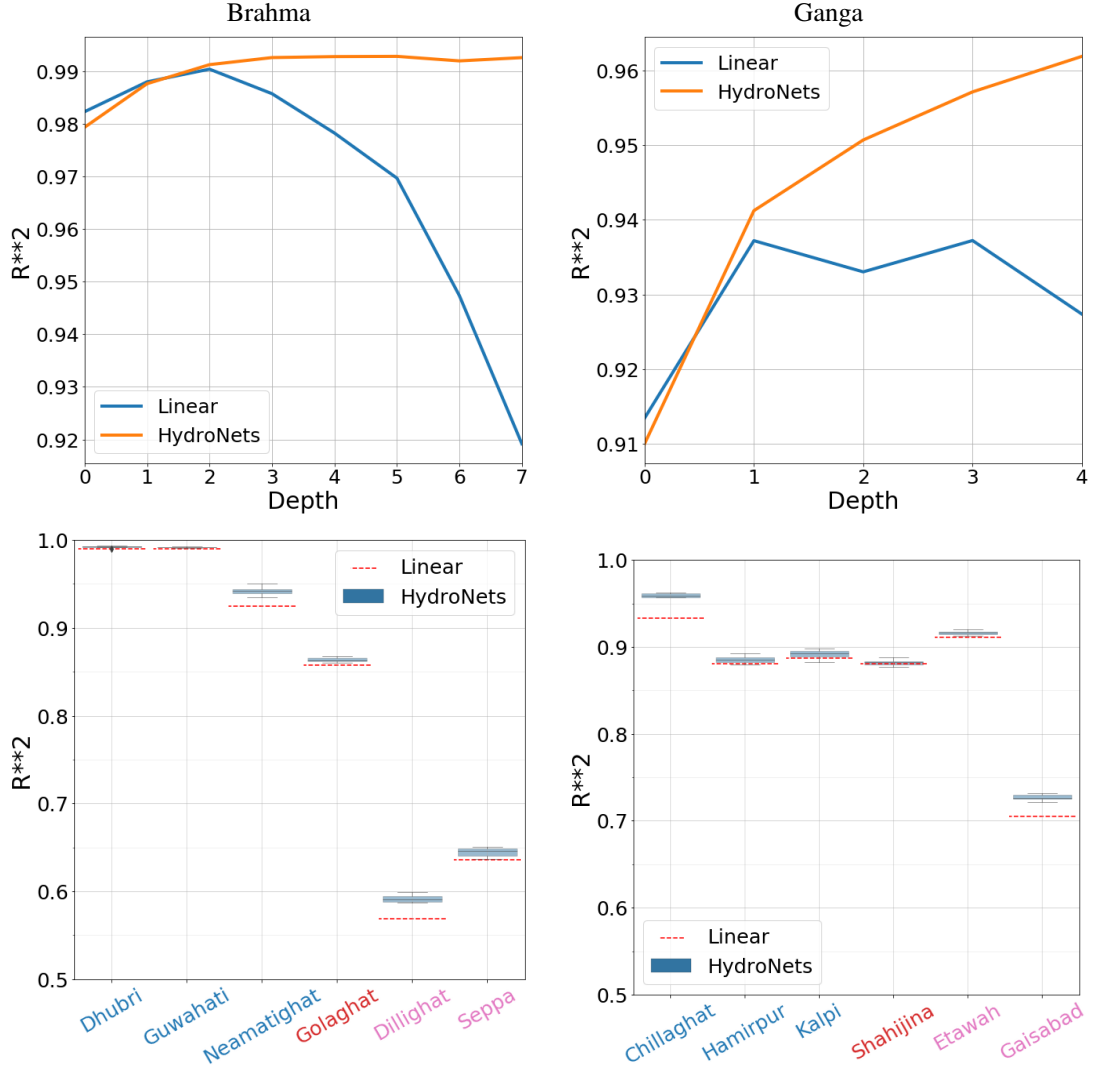

Figure 7: R^2 results